



Investigation of Humidification Dehumidification Water Desalination Integrated with Fogging Technique

Ibrahim M. Nabil^{1*}, Abdalla M. Abdalla¹, Tamer M. Mansour¹, Ali I. Shehata³, Mohamed M. Khairat Dawood²

¹ Faculty of Engineering, Mechanical Engineering Department, Suez Canal University, 44521, Egypt

² Mechanical Engineering Department, Faculty of Engineering, Damanhur University, Elbehira, Egypt

³ Mechanical Engineering Department, Arab Academy for Science, Technology, and Maritime Transport, Alexandria, Egypt

*Corresponding author: Ibrahim M. Nabil, Email address: ibrahim.nabil@eng.suez.edu.eg

DOI: 10.21608/sceee.2025.316740.1039

Article Info:

Article History:

Received: 29\08\2024

Accepted: 10\01\2025

Published: 30\01\2025

DOI: 10.21608/sceee.2025.316740.1039

Abstract

The fogging technique is promising for improving humidification-dehumidification system efficiency and reducing power usage. This research presents an experimental study of a new water desalination system that utilizes a humidification-dehumidification approach. The system is enhanced by including renewable energy sources and a cooling system that integrates a fogging technique. The air is heated using an air conditioning condenser to improve its capacity for effective humidification. Additionally, the fogging system enhances the evaporation process of saline water with a salinity of 34000 ppm. An experimental study investigated the effect of different operational factors such as the mass flow rate ratio, feed water temperatures, and cooling water temperatures on the produced water salinity, desalinated water productivity, efficiency, and cost. The findings indicate that implementing the integrated fogging system has resulted in a higher gain-output ratio and improved desalinated water productivity. The maximum gain output ratio was 8.8 and water productivity was 25 kg/hr. Similarly, the produced water salinity has been lowered from 34000 to 2300 ppm, showing a positive outcome. The water production cost was 0.0088 (\$/liter) for this integrated water desalination system. It is concluded that implementing the integrated fogging system has resulted in higher performance and improved desalinated water productivity.

Keywords: Desalination; Salinity; Humidification-Dehumidification; Water Productivity; Fogging.

Suez Canal Engineering, Energy and Environmental Science Journal (2025), Vol. 3, No.1.

Copyright © 2025 Ibrahim M. Nabil, Abdalla M. Abdalla, Tamer M. Mansour, Ali I. Shehata, Mohamed M. Khairat Dawood. All rights reserved.

1. Introduction

Humidification-dehumidification technology has been empirically demonstrated as a financially efficient method to meet the urgent need for fresh water. Numerous new research inquiries have been undertaken to enhance this technology. The HDH offers several economic and environmental benefits, including the potential to be powered by sustainable energy sources like solar and geothermal, the capacity to operate at low temperatures, reduced maintenance requirements,

How to Cite this Article:

Nabil, I.M. et al. (2025) 'Investigation of Humidification Dehumidification Water Desalination Integrated with Fogging Technique', *Suez Canal Engineering, Energy and Environmental Science Journal*, 3(1), pp. 43–64.

and straightforward building needs. The global water demand is fast increasing due to the substantial population growth. Approximately 97% of the Earth's water is found in the Oceans, while the remaining 3% is freshwater, as depicted in Figure 1. (Gude, 2016; Rosegrant & Cai, 2002)

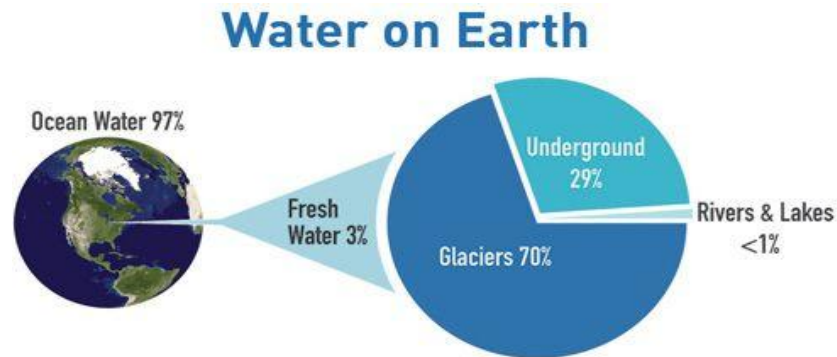


Fig 1. Water distribution (Rosegrant & Cai, 2002).

The lack of fresh water is considered the most crucial issue confronting several places. It is a global concern that coincides with the challenges posed by rapid urbanization, population growth, and economic expansion. The global population is currently experiencing a significant scarcity of clean and fresh water, which is a topic of great concern. Water shortage influences many regions of the world, almost 3.7 billion people are affected (Mohamed et al., 2021). Unfortunately, the population is projected to increase by about 2 billion individuals by 2050. The Population Action International Institute predicts that by 2050, potable water sufficiency, shortage, and stress will be 58%, 18%, and 24%, respectively (Doornbusch et al., 2021).

Numerous desalination technologies have been developed previously. Solar stills are the oldest and most cost-effective means of obtaining pure water. Despite its lack of efficiency, solar stills technology has garnered significant attention from researchers due to its straightforward design and economic benefits. Extensive efforts have been dedicated to the advancement of novel technologies for small-scale water desalination, resulting in the creation of numerous prototypes to verify the feasibility of these innovative concepts (Abu El-Maaty et al., 2023).

While these prototypes may not be the optimal option for competing with existing conventional desalination methods, they do demonstrate their utility in the development of dependable, efficient, and cost-effective decentralized small-scale water desalination systems (Lawal & Qasem, 2020).

The humidification-dehumidification desalination method has gained significant interest in recent years. Due to its notable benefits, extensive research has been conducted on HDH desalination systems, both in theory and through experiments. The fundamental elements of an HDH system comprise a humidifier, a dehumidifier, a water or air heater, pumps, and pipework. Researchers have developed and analysed many designs composed of different components and cycles (Abu El-Maaty et al., 2023).

HDH cycles are commonly classified into water-heated cycles and air-heated cycles based on the kind of heating process, as mentioned in the literature (Alrbai, Enizat, et al., 2022). Furthermore, based on the characteristics of the water and air circulation inside the cycle, they are primarily categorized as closed-water open-air (CWOA), closed-air open water (CAOW), and Open-Air Open Water (OAOW) Systems (Elbassoussi et al., 2021). The components of the HDH system are robust and effectively handle highly salinized water. It is more efficient in treating heavily salinized water than conventional desalination systems. This method has recently been marketed to treat highly salinized water (Nabil et al., 2023).

Solar energy is the promising resource of thermal energy to drive the HDH WDSs in most developing countries that have limited conventional energy resources. The solar energy employed in the seawater desalination processes may be either in the thermal process to provide the thermal energy required or in the membrane desalination processes to generate the required electricity (Santosh et al., 2019). Using solar energy instead of the conventional energy resources in the HDH desalination system to produce fresh water has main advantages such as avoiding freshwater scarcity, using any energy

How to Cite this Article:

resources, high flexibility, reducing greenhouse gas emissions and environmental pollution, and low operating and maintenance costs, while it has a high capital cost (Amran et al., 2020).

HDH systems can be found in two forms: either as standalone systems or integrated with existing thermal systems to enhance their performance. Special emphasis has been placed on integrating the humidification-dehumidification cycles with refrigeration, power, and other desalination technologies in order to improve the efficiency of the combined cycle and increase the quantity of freshwater, cooling capacity, and power output (Chiranjeevi & Srinivas, 2016).

A hybrid absorption cooling device and humidification-dehumidification desalination component has great potential as an energy-saving technology that can reduce energy consumption restrictions (Alkhulaifi et al., 2021). More precisely, out of various methods for recovering waste heat, the idea of combining cooling with humidification-dehumidification processes is a novel approach to create a new thermodynamic system that enhances system performance and productivity (Chiranjeevi & Srinivas, 2016), (Chiranjeevi & Srinivas, 2017).

Implementing the fogging approach in the HDH system will enhance its overall efficiency. This is because the generation of smaller droplets leads to several benefits. Smaller droplets evaporate faster because they have larger areas for heat and mass transmission (Zheng, 2017). As a result, complete evaporation occurs, increasing the system's thermal efficiency. Moreover, the slow speed of these little droplets allows them to enter the flow of air easily. Therefore, the need for larger water flow rates is reduced as the air can efficiently reach saturation. As a result, the humidifier and dehumidifier units are expected to consume less energy while employing the fogging approach to circulate and warm the incoming water (Essa et al., 2024). In addition, the use of lower water flow rates can produce the same level of water production, enabling a more condensed design for the HDH cycle (Chen et al., 2016). Examining the economic aspects of the HDH desalination system is another subject to consider when assessing its potential for commercialization. Cost analysis is a crucial metric for evaluating the efficiency and productivity of the HDH system (Alrbai, Hayajneh, et al., 2022) (Jia et al., 2019).

The costs of desalination are highly challenging to the widespread adoption and commercialization of desalination technology in several different regions. Because the economics of desalination is the primary parameter in the determination of process performance both in the long-term and short-term, various research efforts have addressed costing features of the construction and operation of desalination projects. Most recent studies focus on a particular desalination system or area, which is a possible approach to the estimation of its local costs and environmental effects. On the other hand, the costs associated with water desalination are variable because of technical advancements that have boosted its efficiency and made it more affordable. Even though desalination plants often have a longer lifespan, it is advised that a plant should ideally have a lifespan of twenty years (Delyannis & Delyannis, 1985).

Over the past thirty years, the cost of water desalination has been declining. Desalination technology, feed, and produced water quality, the chosen brine management technique, energy source, and plant location are just a few of the many variables that affect the typical cost of desalinating 1000 gallons of saltwater, which can range from US \$2.00 to \$12.00 (Eke et al., 2020).

The gained output ratio (GOR), which gauges the quantity of freshwater, is one method used to assess the HDH system's performance generated for a specified entropy production and a given heat input (Essa et al., 2024). Accordingly, the effectiveness of the irreversibility of the components is crucial to the HDH system. Consequently, it is necessary to optimize various system components to increase system efficiency including the effect of rust on water quality for potential commercialization (Alrbai, Enizat, et al., 2022).

The use of fogging in HDH water desalination has, as far as we are aware, received little investigation, and this method faces several challenges. Likewise, combining cooling systems with fogging methods. This study aims to enhance the humidification process in desalination systems by including a cooling system integrated with a fogging system. The objective is to investigate the impact of various operating parameters, including cooling water temperature, mass flow rate ratio, and feed water temperature on the performance of the HDH integrated system in terms of water productivity, and gain output ratio. Then compare the results of the new design with other HDH systems.

2. Experimental setup description

The HDH desalination system was installed and subjected to testing at the Faculty of Engineering - Ismailia, Suez Canal University, Egypt.

How to Cite this Article:

Nabil, I.M. et al. (2025) 'Investigation of Humidification Dehumidification Water Desalination Integrated with Fogging Technique', *Suez Canal Engineering, Energy and Environmental Science Journal*, 3(1), pp. 43–64.



Fig. 2. Photos of the actual experimental setup

The design of a novel water desalination system is based on a new approach that utilizes a unit of air conditioning integrated with fogging technique and induction heating.

This system is illustrated in Figure 2. The air is heated using an air conditioning condenser to enhance its capacity for efficient humidification through high-pressure fogging nozzles. A new induction water heating system is employed to heat seawater using the principle of induction heating, which is an appealing solution. The condensation process occurs in a two-stage heat exchanger and the evaporator section of the air conditioning system.

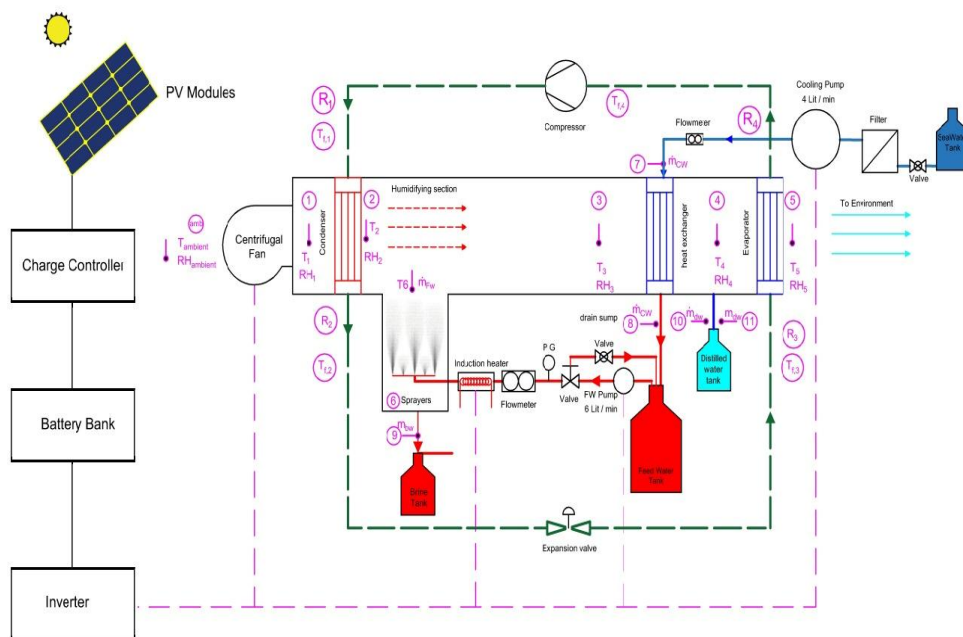


Fig. 3. Schematic diagram of the experimental HDH system setup.

The test rig's specifics and specifications are outlined in the following sections: Airflow system, heating system, humidifying section, dehumidification section, cooling system, distilled water system, solar system, measuring instruments, and test rig description as shown in Figure 3.

How to Cite this Article:

Nabil, I.M. *et al.* (2025) 'Investigation of Humidification Dehumidification Water Desalination Integrated with Fogging Technique', *Suez Canal Engineering, Energy and Environmental Science Journal*, 3(1), pp. 43–64.

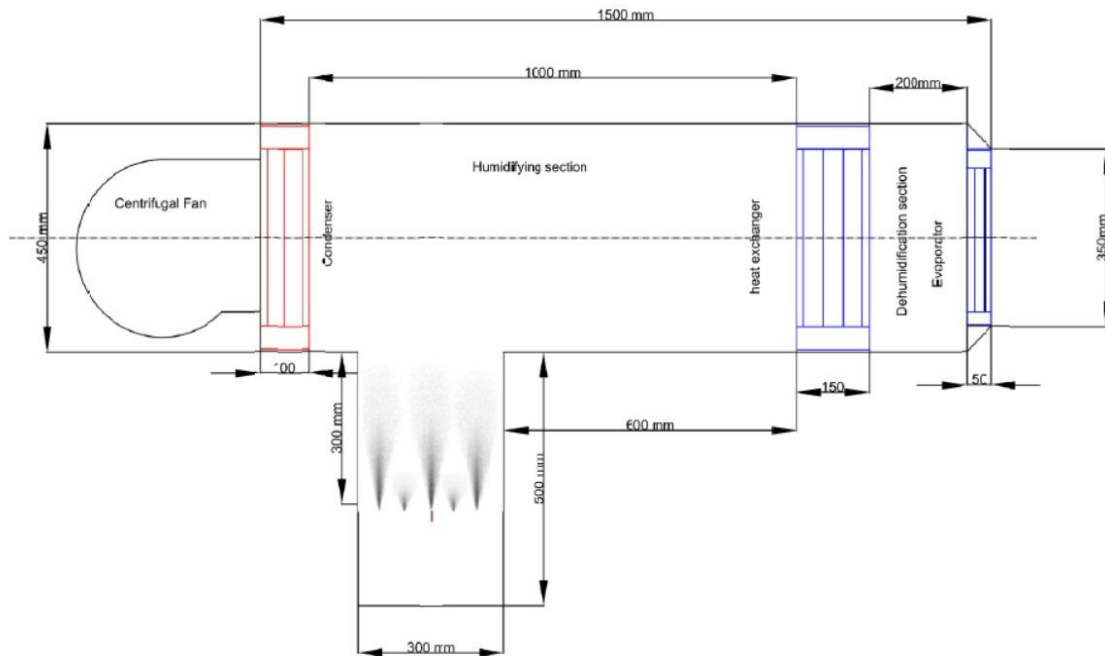


Fig. 4. A schematic drawing with dimensions of the experimental HDH system setup.

The ducts are constructed from galvanized iron sheets with a thickness of 1.5 mm to avoid rusting and promote water quality. These sheets are shaped into rectangular sections of 150 cm in length and have a cross-section of 45x45 cm as shown in figure 4. The ducts are connected to an AC centrifugal fan of the backward-curved, single-intake type, specifically the (R2E220-AB06-05) model, which is powered by the (M2E068-CF) motor. An airflow of 1000 m³/h, with a capacity of 80 W, is utilized to direct air towards the air warmer, humidifier, and dehumidifier. The air velocity is regulated by a dimmer to manage the power input of the fan and maintain the desired air flow rate.

The air is heated using an air conditioning condenser, which consists of a finned tube with dimensions of 450x450x200 mm. The refrigerant Feron (R22) circulates within the copper tubes, while air passes over the external surface of the tubes and fins.

A forced draft fan is utilized to extract air and direct it to the condenser. The purpose of this air is to facilitate the condensation of the refrigerant (R22) through a condenser consisting of finned tubes. As a result of the condenser's rejected heat, the air becomes heated. The flow rate of the air is regulated by a centrifugal fan, with options of 3.4, 6.7, and 10 m³/min.

3. Humidifying section: -

Figure 5. displays the humidification portion, which comprises two ducts. The first part is orientated horizontally and has cross-sectional dimensions of 45*45 cm and a length of 150 cm. Hot air flows through it. The second part is orientated vertically and has cross-sectional dimensions of 30*30 cm and a length of 50 cm. It sprays hot water from the bottom and intersects with the airflow. The ducts are constructed from galvanized sheet metal with a thickness of 1.5 mm. The fogging system comprises a hot water tank with a capacity of 70 liters.

How to Cite this Article:

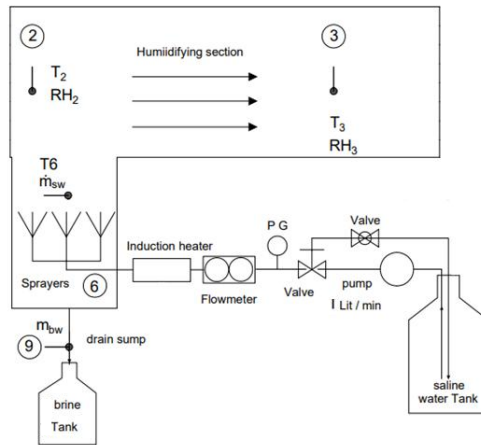


Fig. 5. Schematic Diagram of humidifying section

The apparatus consists of a flexible hose with a diameter of 1/2" and a length of 1.5 meters. It is equipped with a water filter, a high-pressure pump powered by an induction motor (220-240V, 50Hz, 6.5l/min, 1160 psi, 300W), a discharge line made of 3/8" stainless steel, a bath line with valves, a flow meter, and a pressure gauge measuring up to 120 bar. Additionally, there are induction heaters, a high-pressure fogging nozzle with an orifice diameter (0.3mm), and a drain. The ducts' inside is lined with a 1/2 cm thick cork. This cork lining keeps salt from accumulating in the ducts.



Fig. 6. High pressure fogging nozzles

The Fogging system comprises a 3/8-inch stainless-steel pipe located at the bottom of the humidification section. As shown in Figure 6. Six Threadolet 3/16 inches are welded at the end of the stainless-steel pipe 3/8 inches to support six fogging nozzles with a 0.3mm orifice diameter that gives a median droplet size of 8 μm according to the manufacturer's datasheet. The system operates at a pressure range of 30 to 60 bar and the flow rate can be referred to in Table 1.

Table 1. Calibration and Information for Fogging Nozzle

| No. | Des. | Style No. | Orifice | spray | median droplet size | Flow Rate l/min | | | |
|-----|------------------|-----------|---------|-------|---------------------|-----------------|-------|-------|-------|
| | | | Dia | angle | | 30 | 40 | 50 | 60 |
| | | | mm | deg | mic | bar | bar | Bar | bar |
| 1 | FD high pressure | 3010 | 0.3 | 85° | 8 μm | 0.075 | 0.082 | 0.091 | 0.102 |

The primary purpose of the heating system is to warm the water, which is then supplied to the humidifying system to enhance its capacity for vaporization and spraying of the water. Induction Heating System with a Power Output of 120 Watts Coil-equipped Power Supply Module (5V -12V) The power supply has a voltage of 12V and a current of 30A. We

How to Cite this Article:

utilize a pair of stainless-steel pipes with a diameter of 3/8 inch to heat the feed water. The water temperature may be adjusted to 30, 50, or 80 degrees Celsius, depending on the desired temperature and flow rate.

4. Dehumidification section: -

The dehumidification section was constructed using a galvanized iron sheet to avoid rusting and promote water quality with a thickness of 1.5 mm and a cross-sectional area of 45x45x30 cm. A drain is installed in the dehumidifying section to gather the newly formed condensed water during the air dehumidification process, as depicted in Figure 7.

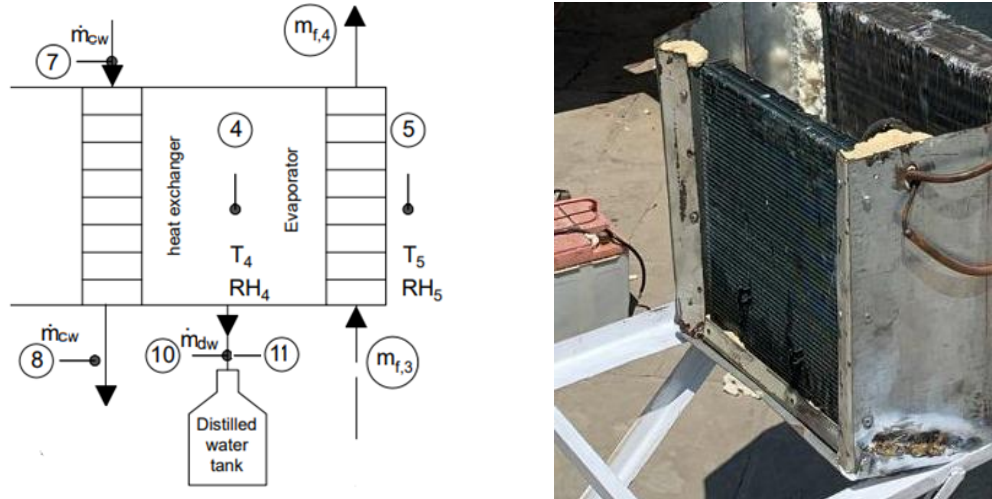


Fig. 7. Schematic Diagram and photo of dehumidification section

The system consists of two stages, the first one by a heat exchanger and the second by an evaporator, as shown in Figure 8. A water-cooled heat exchanger with aluminium finned tubes is fitted. The feed pump delivers water at a rate of 4 liters per minute. The heat exchanger comprises copper tubes with a diameter of 3/8-inch, which are fitted with aluminium fins. The installation of the air condition evaporator has been completed. The evaporator consists of copper coils covered with aluminium fins as shown in Figure 9.

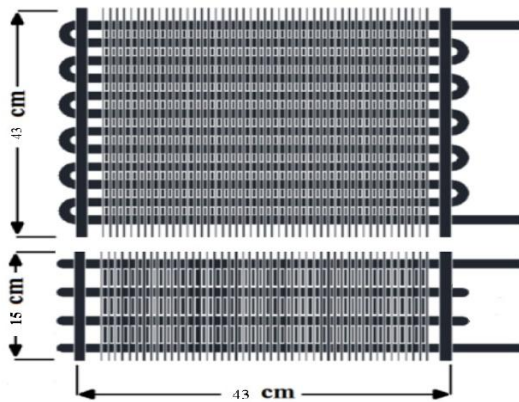


Fig. 8. Schematic Diagram of heat exchanger

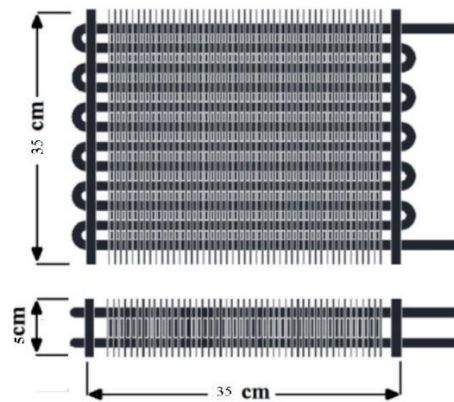


Fig. 9. Schematic of evaporator

5. Solar System: -

The test rig was built and evaluated through multiple experimental testing. solar photovoltaic panels generate electricity for the pumps, the fan, and other auxiliary devices, therefore harnessing a cost-free and environmentally friendly source of energy.

5.1 Photovoltaic solar panels:

How to Cite this Article:

the PV modules of mono-crystalline photovoltaic modules with a max rating power of 300 watt/each and standard test conditions STC (Irradiance 1000 W/m², temperature 25°C) as shown in Figure 10. Each panel contains 60 mono-crystalline, the operating temperature -40 to 85°C.

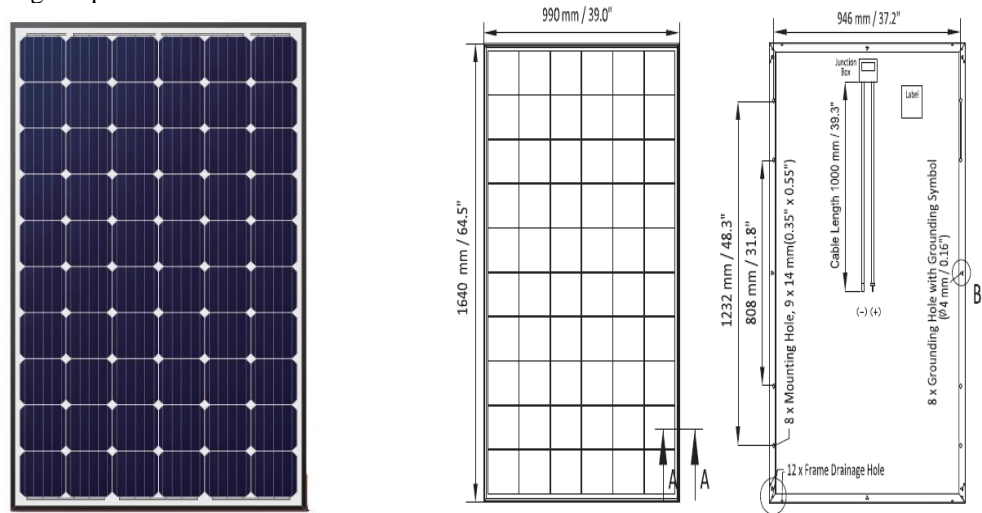


Fig. 10. Schematic of solar panel

The PV array is an interconnection of PV modules or panels that produces direct-current (DC) electricity in direct proportion to the global solar radiation incident upon it, independent of its temperature and voltage to which it is exposed. The PV thermal losses are about 15%. also, the average peak sunshine hour (PSSH) in Ismailia (Egypt) is about 6 hours. These four PV modules' total array peak power is 1176 Watt. To reduce energy consumption, only the energy required for auxiliaries are two pumps, a fan, and one induction heater considered with 8 hours of operation.

5.2 Solar Charge Controller

The charge controller is a regulator which limits the rate of current that goes to and from the battery pack. Charge controllers are essential to prevent overcharging or completely draining a battery. The specification voltage: DC 12V/24V, operating temperature is -35°C-60°C as shown in Figure 11.

5.3 Batteries Storage

Two batteries of 840 Wh (70 Amp*12V) connected in series are selected, producing 1680 W hour (70 Amp*24V). The battery bank can operate the HDH unit continuously for approximately 2.24 hours under full load before it needs recharging.

5.4 Inverter:

An inverter converts the DC electricity stored in the batteries to AC power, which is required for operating AC-powered devices within the HDH (Humidification-Dehumidification) test rig. The inverter's capacity should match the peak power requirements of the HDH system.

The inverter must be rated to handle peak power consumption, especially during induction heater operation. Inverter Rating: 1000W continuous, 24V to 220V AC.

How to Cite this Article:

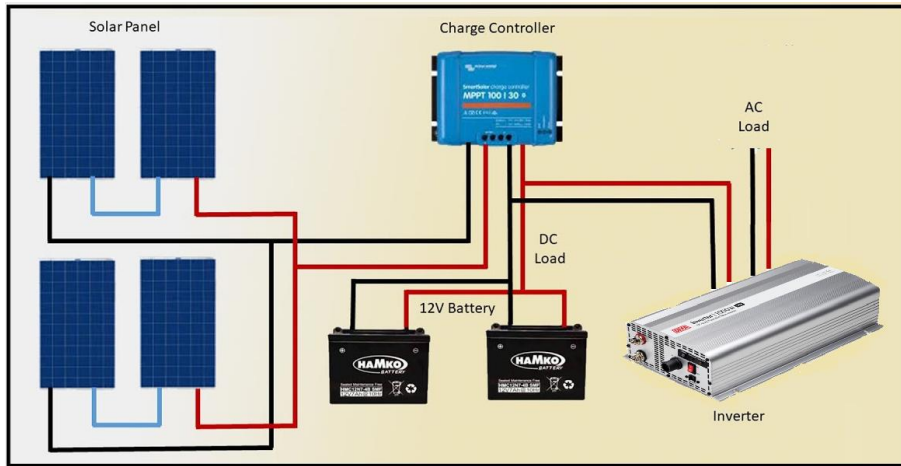


Fig. 11. Schematic diagram of Photovoltaic Solar Panel Module integrated with HDH System

6. Test Rig steps description: -

A cooling water system, a hot water system, and an air system make up the test rig setup. Twenty minutes were allotted for the test runs to achieve steady-state boundary conditions. A calibrated tank is used to measure and dispose of the condensate, and the output distillate was monitored hourly.

The start-up procedures for the experimental apparatus are described as follows:

- Based on the previous calibration data, the water pumps and the fan are adjusted by their regulating appliances at the required flow rates.
- The feed water is heated to (30, 50, and 80°C) through the heating system. This requires determining the number of heaters and the heating duration to maintain the water temperature before entering the fog nozzles.
- Once the air temperature is steady, the hot water starts fogging water, and cold water is directed to the heat exchanger and both the humidifying system and dehumidifying system to start full operation.
- At the same moment as the experiment starts fully operating, the temperature of refrigerant R22 at the inlet and outlet of the condenser and evaporator are noted and recorded.
- Ambient temperature, Air velocity as well as water temperature, and flow mass rate readings are noted and recorded.

The test run was expanded over 8 hours of operation time under invariant inlet and boundary conditions. During experimentation, the mass flow meters were checked regularly every 30 minutes, and the output distillate was noted and recorded every half an hour.

Table 2. Different studying parameters.

| No. | Parameter | Unit |
|-----|--|--------|
| 1 | The mass flow rate of feed water (m_{fw}) | kg/min |
| 2 | Temperature of feed water (T_{fw}) | ° C |
| 3 | The mass flow rate of cooling water (m_{cw}) | kg/min |
| 4 | Temperature of cooling water (T_{cw}) | ° C |
| 4 | Mass flow rate of air (m_{air}) | Kg/min |
| 5 | Air velocity (V_a) | m/s |
| 6 | Operating pressure (P_{hw}) | bar |
| 7 | Mass flow rate ratio (m_{fw}/m_{air}) | |
| 8 | Salinity of feed water | ppm |

7. Measuring devices and error analysis

Based on information from the measuring instrument specification data sheet, Table 3 displays the accuracy and range of each measuring device.

Table 3. Experimental measuring instruments with range and accuracy

| Measuring Instrument | Parameter | Range | Accuracy |
|-----------------------------------|---------------|----------------|-----------|
| Digital Thermometer Sensor LCD | temperature | -50 ~ 110 °C | ± 0.1 °C |
| Temperature K-type thermocouple | temperature | -270 to 1260°C | ±0.2°C |
| Air Flow Speed (Anemometer UT363) | Air flow rate | 0-30 m/s | ± 0.1 m/s |

How to Cite this Article:

Nabil, I.M. et al. (2025) 'Investigation of Humidification Dehumidification Water Desalination Integrated with Fogging Technique', *Suez Canal Engineering, Energy and Environmental Science Journal*, 3(1), pp. 43–64.

| | | | |
|---|-------------------|---------------|------------------------------|
| Water Flowmeter FL-408 | Water flow rate | 1 to 30 l/min | ± 0.5 l/min |
| Humidity Sensor HTC-2 | Humidity ratio | 10-99 % RH | ± 1 % RH |
| Jenway 4520 Conductivity /TDS /Resistivity/Salinity Meter Kit | Water salinity | 0 to 99.9 g/L | 0-35 ±1g/L, 35-99.9 ±3g/L |
| solar intensity solarimeter | solar intensity | 0–5000 W/m2 | ±5W/m2 |
| Distilled water (graduated tank) | Desalinated water | 0–5000mL | ±50 mL |

The parameters that influence the system’s performance are observed experimentally.

The uncertainties of the calculations are based on ANSI/ASME standard (Abemethy et al., 1983) using Eq. (1).

$$w_R = \sqrt{\left[\left(\frac{\partial R}{\partial x_1} w_1\right)^2 + \left(\frac{\partial R}{\partial x_2} w_2\right)^2 + \left(\frac{\partial R}{\partial x_3} w_3\right)^2 + \dots + \left(\frac{\partial R}{\partial x_n} w_n\right)^2\right]} \quad (1)$$

Where: -

R=Inputs functions (x_1, x_2, \dots, x_n)

w_1, w_2, \dots, w_n = refers to the uncertainties of these variables.

w_R =Cumulative uncertainty.

8. Experimental procedure

An experiment was carried out in Ismailia, Egypt, over the three summer months of 2023, from 8 A.m. to 4 P.m., to study the effects of humidification and dehumidification on the water desalination system. Every experiment conducted has an average duration of three days per month.

Table 4. The experimental parameters and values.

| No. | Parameter | Unit | value |
|-----|--|---------------------|------------------------------|
| 1 | Refrigerant R22 flow rate | Kg/s | 0.02 |
| 2 | Mass flow rate of air | Kg/min | 4, 8, 12 |
| 3 | Air flow rate | m ³ /min | 3.4, 10 |
| 4 | Mass flow rate of feed water for orifice nozzle diameter 0.3mm | Kg/min | 0.45, 0.492, 0.546, 0.612 |
| 5 | Mass flow rate of cooling water | Kg/min | 4 |
| 6 | Salinity of feed water | ppm | 34,000 |
| 7 | Temperature of feed water | ° C | 30, 50, 80 |
| 8 | Temperature of cooling water | ° C | 22, 20, 18 |

9. Data reduction and government equations:

As shown in Figure 12 shows a process flow diagram of the integrated HDH water desalination system, The system consists of four cycles: one cycle for air and two cycles for water (one for hot feed water and the second for cooling water), and the last one for the refrigerant circuit using Freon R22. The refrigerant circuit and heating are powered by electricity and the initial heating and condensing circuits are powered by solar cells.

How to Cite this Article:

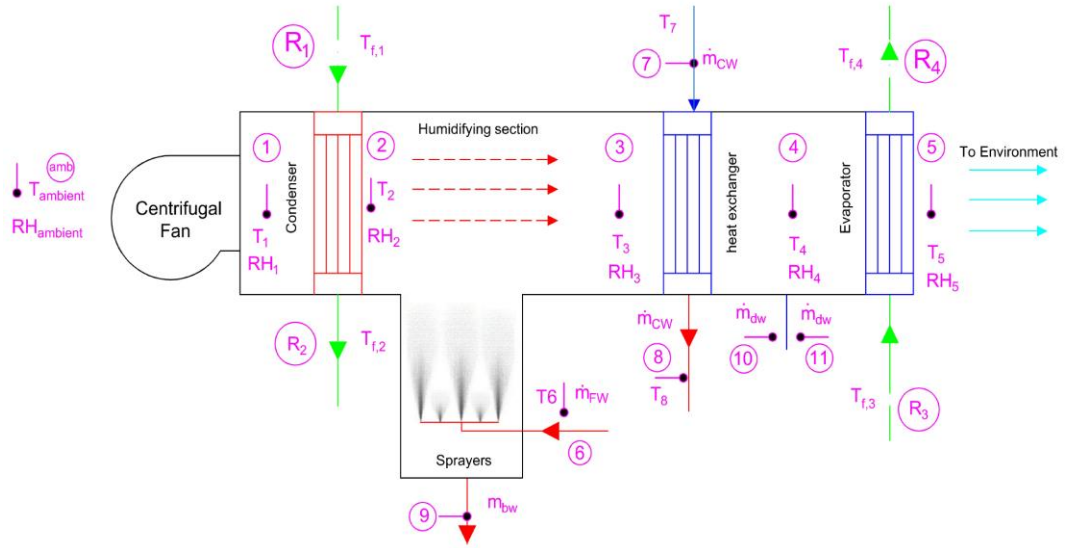


Fig. 12. Process flow diagram of HDH Water Desalination System

Where: -

| | | | |
|-----------|--|-----------|---|
| T_{amb} | Ambient Temperature | $T_{f,1}$ | The inlet temperature of R22 to Condenser |
| T_1 | Air Temperature inlet to condenser | $T_{f,2}$ | Outlet temperature of R22 from Condenser |
| T_2 | Air Temperature outlet from condenser | $T_{f,3}$ | The inlet temperature of R22 to Evaporator |
| T_3 | Saturated air Temperature outlet from humidifier | $T_{f,4}$ | Outlet temperature of R22 from Evaporator |
| T_4 | Air Temperature outlet from the first dehumidifier | RH_1 | Air relative humidity inlet to Condenser |
| T_5 | Air Temperature outlet of the second dehumidifier | RH_2 | Air relative humidity outlet from Condenser. |
| T_6 | Water Temperature inlet to humidifier. | RH_3 | Air relative humidity inlet to Heat Exchanger. |
| T_7 | Water Temperature inlet to heat exchanger. | RH_4 | Air relative humidity outlet from Heat Exchanger. |
| T_8 | Water Temperature outlet from heat exchanger | RH_5 | Air relative humidity inlet to Evaporator. |

9.1 Air Heater (Condenser):

The air heater has an Energy Balance applied to it.

$$\dot{m}_{air,1} h_1 + \dot{m}_{f,1} h_{f,1} = \dot{m}_{air,2} h_2 + \dot{m}_{f,2} h_{f,2} \quad (2)$$

Where: -

| | | | |
|-------------------|---|-----------------|---|
| $\dot{m}_{air,1}$ | The mass flow rate of inlet air to the condenser | $\dot{m}_{f,1}$ | The mass flow rate of inlet refrigerant to the condenser |
| $\dot{m}_{air,2}$ | The mass flow rate of exit air from the condenser | $\dot{m}_{f,2}$ | The mass flow rate of exit refrigerant from the condenser |
| h_1 | Enthalpy of inlet air to condenser | $h_{f,1}$ | Enthalpy of refrigerant inlet to condenser |
| h_2 | Enthalpy of exit air from the condenser | $h_{f,2}$ | Enthalpy of refrigerant exit from condenser |

9.2 Humidifying Section (Humidifier):

In the humidifier, the fogging of seawater is in direct contact with dry air withdrawing the air heater. Therefore, Energy and mass balance are applied to the humidifier as shown in Figure 13.

How to Cite this Article:

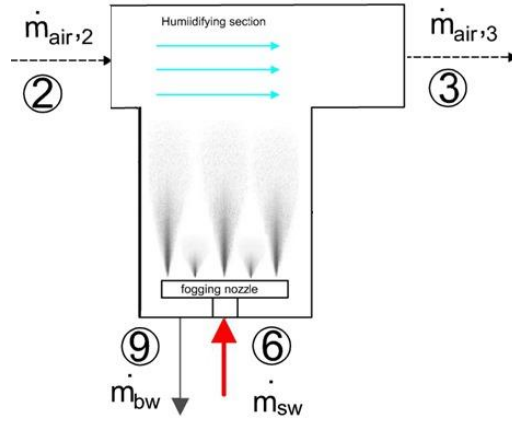


Fig. 13. Energy and mass balance of Humidifying section

The energy and mass balance in the humidifier:

$$\dot{m}_{air,2} h_2 + \dot{m}_{sw,6} h_6 = \dot{m}_{air,3} h_3 + \dot{m}_{b,w} h_9 \quad (3)$$

$$\dot{m}_{sw,6} + \dot{m}_{air,2} \omega_2 = \dot{m}_{b,w} + \dot{m}_{air,3} \omega_3 \quad (4)$$

Where: -

| | | | |
|-------------------|---|------------|--|
| $\dot{m}_{air,3}$ | The mass flow rate of inlet air to the heat exchanger | h_3 | Enthalpy of inlet air to the heat exchanger |
| $\dot{m}_{sw,6}$ | The mass flow rate of inlet hot seawater | h_6 | Enthalpy of inlet hot seawater |
| $\dot{m}_{b,w}$ | The mass flow rate of brine water | h_9 | Enthalpy of brine water |
| ω_2 | Specific humidity of exit air from the condenser | ω_3 | Specific humidity of inlet air to heat exchanger |

9.3 Dehumidifying Section (Heat Exchanger):

In the first dehumidifying section the energy and mass balance are applied.

$$\dot{m}_{air,3} h_3 + \dot{m}_{cw,7} h_7 = \dot{m}_{air,4} h_4 + \dot{m}_{cw,8} h_8 + \dot{m}_{dw,10} h_{10} \quad (5)$$

$$\dot{m}_{cw,7} = \dot{m}_{cw,8} \quad (6)$$

$$\dot{m}_{dw,10} = \dot{m}_{air,3} (\omega_3) - \dot{m}_{air,4} (\omega_4) \quad (7)$$

Where: -

| | | | |
|-------------------|---|----------|--|
| $\dot{m}_{air,4}$ | The mass flow rate of inlet air to the heat exchanger | h_4 | Enthalpy of exit air from heat exchanger |
| $\dot{m}_{cw,7}$ | The mass flow rate of inlet cooling water | h_7 | Enthalpy of inlet cooling water |
| $\dot{m}_{cw,8}$ | The mass flow rate of exit cooling water | h_8 | Enthalpy of exit cooling water |
| $\dot{m}_{dw,10}$ | The mass flow rate of first desalinated water | h_{10} | Enthalpy of first desalinated water |
| ω_4 | Specific humidity of exit air from the heat exchanger | | |

9.4 Dehumidifying Section (Evaporator):

In the second dehumidifier energy and mass balance is applied.

$$\dot{m}_{air,4} h_4 + \dot{m}_{f,3} h_{f3} = \dot{m}_{air,5} h_5 + \dot{m}_{f,4} h_{f4} + \dot{m}_{dw,11} h_{11} \quad (8)$$

$$\dot{m}_{air,4} \omega_4 = \dot{m}_{air,5} \omega_5 + \dot{m}_{dw,11} \quad (9)$$

Where: -

| | | | |
|-------------------|--|-------|--|
| $\dot{m}_{air,5}$ | The mass flow rate of exit air from the evaporator | h_5 | Enthalpy of exit air from the evaporator |
|-------------------|--|-------|--|

How to Cite this Article:

| | | | |
|-------------------|--|-----------|---|
| $\dot{m}_{f,3}$ | The mass flow rate of inlet refrigerant to evaporator | $h_{f,3}$ | Enthalpy of the refrigerant inlet to the evaporator |
| $\dot{m}_{f,4}$ | The mass flow rate of exit refrigerant from the evaporator | $h_{f,4}$ | Enthalpy of refrigerant exit from evaporator |
| $\dot{m}_{dw,11}$ | The mass flow rate of the second desalinated water | h_{11} | Enthalpy of second desalinated water |
| ω_5 | Specific humidity of exit air from the evaporator | | |

The total productivity of desalinated water collected from the HDH desalination unit is shown in the following equation:

$$\dot{m}_{total\ produce} = \dot{m}_{dw,10} + \dot{m}_{dw,11} \quad (10)$$

9.5 Water Heater:

The total heat input given to the saline feed water is equal to the sum of energy generated by the induction heaters and energy available for heat recovery coming from the first dehumidifier at point 8 hot saline water tank.

$$\dot{Q}_{in} = \dot{m}_{sw,6}(h_6 - h_8) \quad (11)$$

$$h_6 = C_p T_6 \quad (12)$$

The amount of thermal power in watts transmitted to water can be determined by the formulation (Korepanov et al., 2020):-

$$P_w = \dot{m}_{sw,6} * C_{pw} * (T_6 - T_8) * \frac{1}{3.6 * t} \quad (13)$$

where, C_{pw} - average heat capacity of water, KJ/kg·K; t is the time of heating water from temperature T_8 to T_6 , hours.

9.6 Gain Output Ratio (GOR):

The daily efficiency of the fog-desalination process or thermal performance of the HDH desalination system was evaluated by GOR. That is defined as the ratio of the latent heat of evaporation of the freshwater produced to the total energy input into the HDH desalination system (El-Maaty et al., 2019) and (El-Maaty et al., 2024).

$$GOR\ or\ \eta_{fp} = \frac{\Sigma(m_{condense} h_{fg})}{\Sigma P_w + 3(W_{fan} + W_{p1} + W_{p2} + W_{comp}) \Sigma \Delta t} \quad (14)$$

9.7 Mass Flow Rate Ratio (MR):

The mass flow rate ratio is defined as the ratio of the water mass flow rate to the circulating dry air mass flow rate in the cycle (Sharqawy et al., 2014).

$$MR = \frac{\dot{m}_{sw,6}}{\dot{m}_{air}} \quad (15)$$

10. Economic evaluation and cost analysis

The desalination unit could produce up to 203 liters/day with a fogging nozzle of 0.3mm. Table 5. Shows the cost analysis of the system specification and economic assumptions.

Table 5 Economic considerations

| | |
|----------------------------|------------------|
| Water production | 203 liters/day |
| Electrical input | 28.672 kWh/day |
| Solar system output | 5.2 kWh/day |
| Interest rate (<i>i</i>) | 20 % |
| power Cost | 0.031 \$ per kWh |
| preservation | 15 % |
| Lifetime | 10 years |

How to Cite this Article:

The desalination unit generates a maximum of 203 liters of desalinated water daily. The system operates for 8 hours every day. The annual desalinated water output with a nozzle diameter of 0.3 mm is 69,020 liters, The estimated lifespan is 10 years. The economics of the intended HDH desalination system are evaluated using an annualized cost technique (Fath et al., 2003).

The following calculation factors may be expressed as: -

$$CRF = \frac{i(1+i)^n}{(1+i)^n - 1} \quad (16)$$

$$FAC = P \times CRF \quad (17)$$

The salvage value of the system after the lifetime (n = 10 years) equals 20% of the total fixed cost. The sinking fund factor (SFF) and the annual salvage value (ASV) are calculated according to (Jamil et al., 2018).

$$SFF = \frac{1}{(1+i)^n - 1} \quad (18)$$

$$S = 0.2 \times P \quad (19)$$

$$ASV = SFF \times S \quad (20)$$

The maintenance yearly cost (AMC) is assumed to be 15% of the fixed annual cost as follows:

$$AMC = 0.15 \times FAC \quad (21)$$

The yearly running cost of power consumption used in the system: -

$$ARC = Power \times CEH \times 8 \times 340 \quad (22)$$

CEH is the Cost of Electricity, \$ Per kWhr

The yearly cost (AC) is estimated as follows:

$$AC = FAC + AMC + ARC - ASV \quad (23)$$

Finally, the cost per liter (CPL) is given by:

$$CPL = \frac{AC}{M} \quad (24)$$

The capital cost analysis of the HDH desalination unit is shown in Table 6. The different expenses include wiring, consumable components, and transportation. The specified cost per liter of the system is shown in Table 7. The cost of water delivery is \$0.0088 per liter. Table 8 presents a comparative analysis of the prior research studies. (Shehata et al., 2019), (Khairat Dawood et al., 2021). The suggested system has a reduced cost compared to the others, achieving an annual output of 69,020 liters.

Table 6 Capital cost of HDH desalination unit

| Item description | Unit price \$ | Quantity | Total cost \$ |
|-------------------------------|---------------|----------|---------------|
| Centrifugal fan | 58 | 1 | 58 |
| High-pressure water pump | 82 | 1 | 82 |
| Cooling water pump | 25 | 1 | 25 |
| Humidifier (condenser) | 35 | 1 | 35 |
| Dehumidifier (evaporator) | 25 | 1 | 25 |
| Dehumidifier (heat exchanger) | 50 | 1 | 50 |
| Compressor R22 | 49 | 1 | 49 |
| Piping and fittings | 25 | 1 | 25 |
| Control unit | 51 | 1 | 51 |

How to Cite this Article:

| | | | |
|------------------------------|-----|---|------|
| Fogging nozzle | 40 | 1 | 40 |
| Ducts | 30 | 1 | 30 |
| Water Tanks | 25 | 2 | 50 |
| Solar panels with cables | 100 | 4 | 400 |
| Solar charger controller | 80 | 1 | 80 |
| Battery | 80 | 2 | 160 |
| Inverter with cales | 50 | 1 | 50 |
| distribution board | 20 | 1 | 20 |
| Miscellaneous | 20 | 1 | 20 |
| Installation and fabrication | 60 | 1 | 60 |
| Capital Cost (P) \$ | | | 1300 |

Table 7. Cost of distilled water per liter of HDH desalination unit

| Item | Cost, \$ |
|--|-------------------|
| Total capital cost | 1300 |
| Capital recovery factor (CRF) | 0.2385 |
| Fixed annual cost (FAC) | 310.05 |
| Sinking fund factor (SFF) | 0.192 |
| Salvage value (S) | 260 |
| Annual salvage value (ASV) | 49.92 |
| Annual maintenance cost (AMC) | 46.5 |
| Annual cost of power (ARC) (0.3 mm) | 302.2 |
| The yearly cost (AC)(0.3mm) | 608.83 |
| Cost of desalinated water per liter (CPL) (0.3 mm) | 0.0088 (\$/liter) |

Table 8. Comparison between the current work and similar works.

| Study | HDH Configuration | Feed water Temp. (°C) | Energy source | Energy Consumption | Maximum Productivity | Cost per liter (\$/L) |
|---|-------------------|-----------------------|----------------|--------------------|----------------------|-----------------------|
| Current research work | OAOW-WH, AH | 30 - 80 °C | Electric+Solar | 3.584 Kwh | 25 L/h | 0.0088 |
| Shehata et al.(Shehata et al., 2019) | OAOW-WH, AH | 60 °C | Electric+Solar | 8.5 Kwh | 3.67 kg/h | 0.0144 |
| Khairat Dawood et al. (Khairat Dawood et al., 2021) | OAOW-WH, AH | 90 °C | Solar+Gas | 4 KWh | 3.52 L/h | 0.01141 |

11. Results: -

This study examines the experimental application of fogging saline water in water desalination. An experimental study was conducted to investigate the relationship between the mass flow rate ratio, inlet cooling water temperature, and feed water temperature, and their impact on the productivity of distilled water, the salinity of the product water, and the performance of the fog-desalination process. The results are presented in the following figures:

11.1 Effect of mass flow rates ratio on produced desalinated water with different FWT

How to Cite this Article:

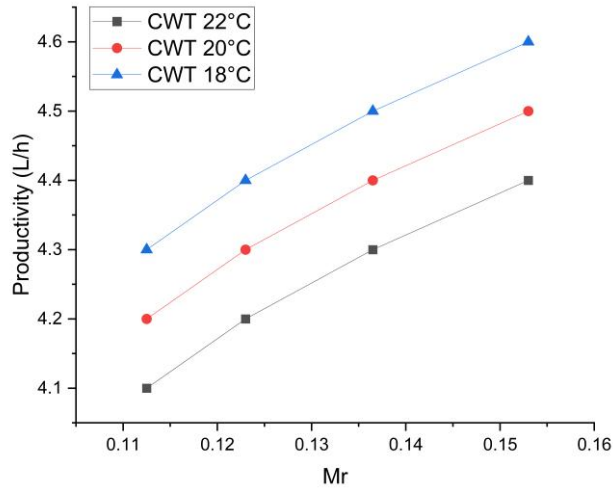


Fig.14. Relation of Mr and productivity with air flow rate 3.4 m³/min, FWT 30°C and FWS 34000 ppm at different CWT.

Figure 14. shows the relation between water productivity (in liters per hour, L/h) and the mass flow rate ratio (Mr). At an airflow rate of 3.4 m³/min, feed water salinity (FWS) is fixed at 34,000 ppm parts per million, while the feed water temperature (FWT) is kept at 30°C. with three different cooling water temperatures (CWT): 22°C, 20°C, and 18°C.

Productivity increases with Mr at all CWT values, indicating a direct relationship between water productivity and the mass flow rate ratio. The best productivity is with lower CWT. This implies that lower cooling temperatures increase the system's efficiency, most likely due to improved heat exchange efficiency.

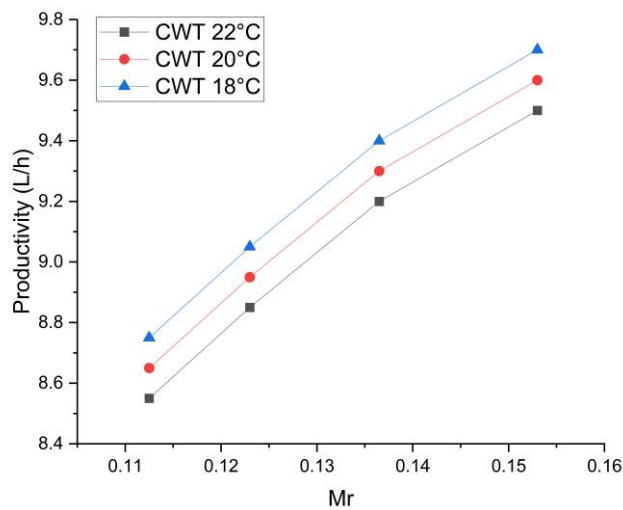


Fig.15. Relation of Mr and productivity at air flow rate 3.4 m³/min, FWT 80°C at different CWT.

Figure 15. Shows the relation between water productivity (in liters per hour, L/h) and the mass flow rate ratio (Mr). At an airflow rate of 3.4 m³/min, feed water salinity (FWS) is fixed at 34,000 ppt parts per million, while the feed water temperature (FWT) is kept at 80°C. with three different cooling water temperatures (CWT): 22°C, 20°C, and 18°C.

Compared to Figure 1 with an FWT of 30°C, this system design (higher FWT of 80°C) produces greater productivity. Evaporation rates and overall performance are probably enhanced by the increased feed water temperature. The crucial impact that feed and cooling water temperatures have on system efficiency is highlighted by this research.

How to Cite this Article:

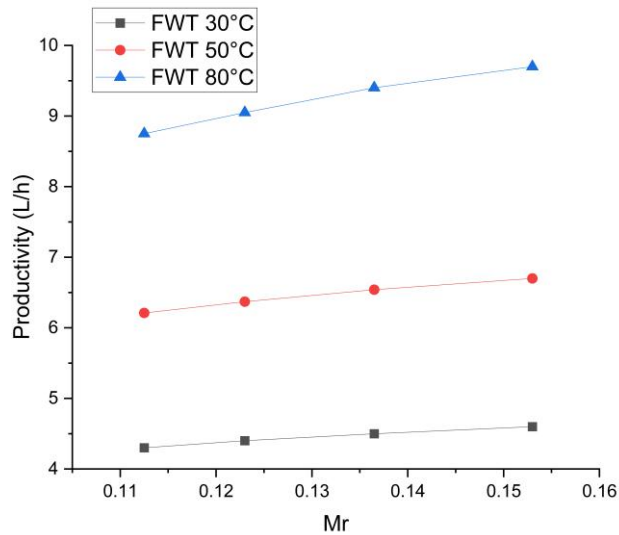


Fig.16. Relation of Mr and productivity at air flow rate 3.4 m³/min, CWT 18°C at different FWT.

Figure 16. illustrates the connection between the mass flow rate ratio (Mr) and productivity (L/h) with a cooling water temperature (CWT) of 18°C and the feed water temperature (FWT) set at 30°C, 50°C, and 80°C at an airflow rate 3.4 m³/min. Higher FWT values lead to dramatically increased productivity at any given Mr. This is because higher feed water temperatures increase evaporation rates, which improves system performance. The feed water temperature (FWT) is critical in determining the system's efficiency. Higher FWT values significantly increase performance, highlighting the need of preheating input water in high-productivity applications.

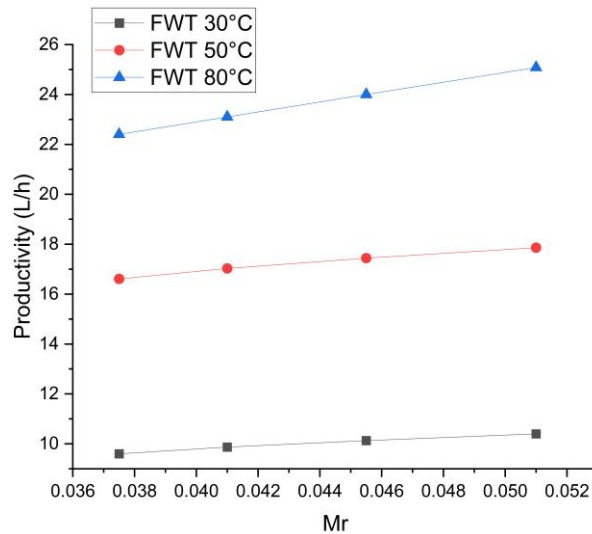


Fig.17. Relation of Mr and productivity at air flow rate 10 m³/min, CWT 18°C at different FWT.

Figure 17. illustrates the connection between the mass flow rate ratio (Mr) and productivity (L/h) with a cooling water temperature (CWT) of 18°C and the feed water temperature (FWT) set at 30°C, 50°C, and 80°C at an airflow rate 10 m³/min. Higher FWT values lead to dramatically increased productivity at any given Mr. The airflow rate has a substantial influence on water production in desalination operations. The airflow rate influences the humidification and dehumidification processes. The maximum water productivity was 25 kg/hr Higher airflow rates can increase the quantity of water vapor transported by the air, resulting in more freshwater productivity.

11.2 Effect of mass flow rates ratio produced water salinity at different FWT

How to Cite this Article:

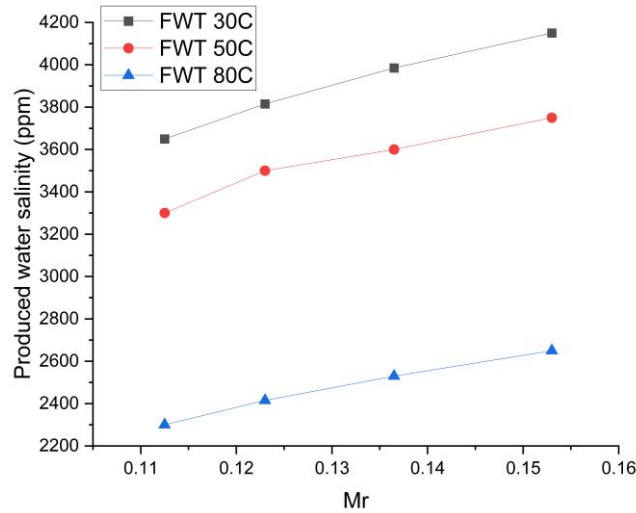


Fig.18. Relation of Mr and produced water salinity at air flow rate 3.4 m³/min at different FWT.

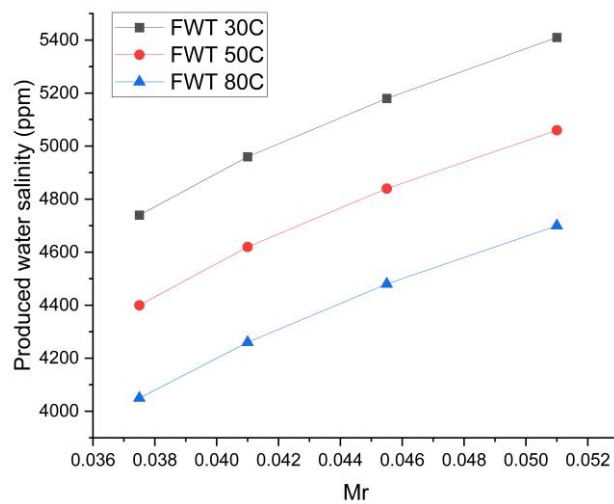


Fig.19. Relation of Mr and produced water salinity at air flow rate 10 m³/min at different FWT.

Figure 19 depicts the relationship between the mass flow rate ratio and the salinity of produced water, measured in parts per million. The experiment was carried out by manipulating different feed water temperatures. The salinity of the water produced decreased by about 88% as it decreased from 34000 ppm to 4050 ppm at 80 °C.

11.3 Effect of mass flow rates ratio on GOR at different FWT.

How to Cite this Article:

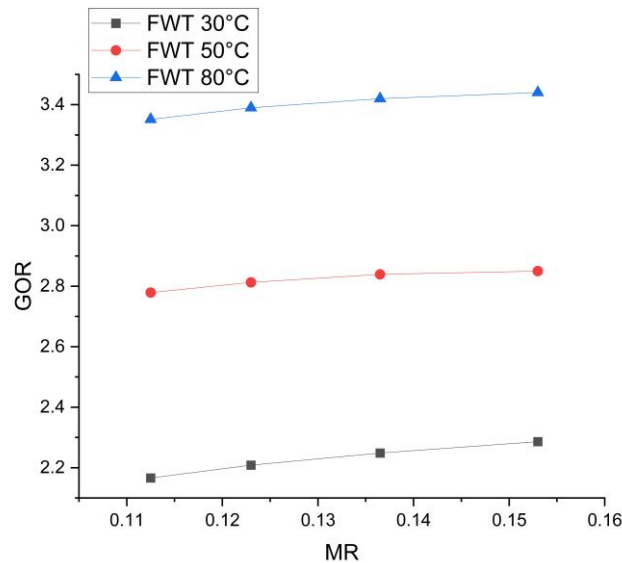


Fig.20. Relation of Mr and GOR at air flow rate 3.4 m³/min, CWT 18°C, and at different FWT.

Figure 20. depicts the correlation between MR and GOR for fogging nozzles with specific parameters (0.3 mm nozzle size, air flow rate of 3.4 m³/min, and cooling temperature of 18°C) under varying feed water salinities. The gain output ratio (GOR) is a metric of desalination process efficiency that is defined as the ratio of the mass of distilled water produced to the mass of water input. It displays how well the system transforms feed water into distilled water. In general, an increase in feedwater temperature leads to an increase in GOR. The rise in GOR persists as the feed water mass flow rate increases.

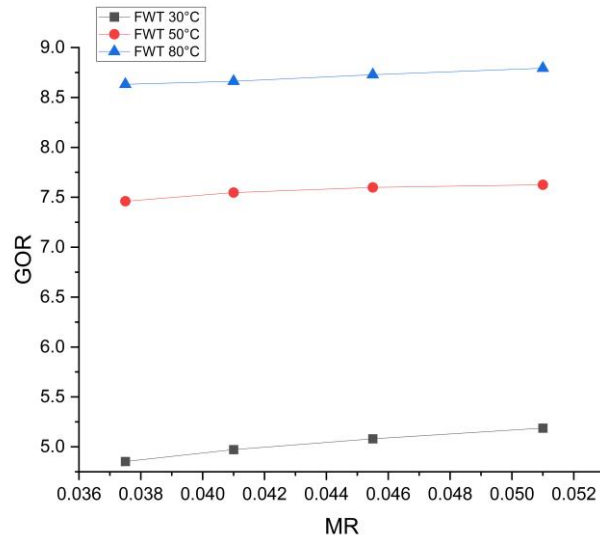


Fig.21. Relation of Mr and GOR at air flow rate 10 m³/min, CWT 18°C, and FW salinity at different FWT.

Figure 21. depicts the correlation between MR and GOR for fogging nozzles with specific parameters (air flow rate of 10 m³/min, and cooling temperature of 18°C) under varying feed water salinities. In general, an increase in feedwater temperature leads to an increase in GOR. The rise in GOR persists as the feed water mass flow rate increases. The maximum gain output ratio was 8.4. The rise in GOR signifies an improvement in the effectiveness of the desalination process per unit. GOR varies directly with productivity and inversely with consumed power. Hence, the GOR value is affected by the system's operational parameters and energy consumption during operation.

How to Cite this Article:

12. Conclusions

The most important conclusions of the experimental study are outlined below:

- The optimal salinity of the produced water was 2300 parts per million (ppm) using a fogging nozzle with an orifice diameter of 0.3 mm, operating at a pressure of 30 bar and a temperature of 80°C. The input water had a salinity of 34,000.
- The system can lower the amount of total dissolved solids from 34,000 parts per million (ppm) to 2300 ppm, 3300 ppm, and 3650 ppm when the feed water temperatures are 80°C, 50°C, and 30°C, respectively, according to salinity analyses.
- The water productivity reaches a maximum value of 25 liter/h with a feed water salinity of 34,000 ppm and an airflow rate of 10 m³/min, using a fogging nozzle with an orifice diameter of 0.3 mm.
- The maximum GOR was 8.8 for a feed water salinity of 34,000 ppm when the airflow rate was 10 m³/min.
- Feed and cooling water temperatures have a great impact on system performance in this research
- The airflow rate significantly affects the performance of the fog-integrated system.
- An economic cost analysis revealed that the cost per liter for the distilled water product is \$/L 0.0088, which competes with previous work.

NOMENCLATURE

| Symbols | Description | Symbols | Description |
|---------|-----------------------------------|----------------|------------------------------|
| AC | The yearly cost \$ | \dot{m} | Mass Flow rate kg/s |
| AMC | Annual maintenance cost \$ | MR | Mass flow rate Ratio |
| ARC | Annual cost of power \$ | n | Lifetime Years |
| ASV | Annual salvage value \$ | OACW | Open Air Closed Water |
| Cp | Specific heat capacity kJ/kg.oC | OAOW | Open Air Open Water |
| CAOW | Closed air open water | OARO | Osmotically assisted RO |
| CPL | Cost Per Liter \$ | P | Present Capital Cost \$ |
| CRF | Capital Recovery Factor | P_w | Consumable power kW |
| CWT | Cooling water temperature oC | ppm | Parts per million |
| FAC | Fixed Annual Cost \$ | PV | Photovoltaic |
| FWT | Feed Water Temperature oC | \dot{Q}_{in} | Heat rate input kW |
| GOR | Gain Output Ratio | RH | Relative humidity |
| H | Specific enthalpy kJ/kg | S | Salvage value |
| hfg | Latent heat of vaporization kJ/kg | SFF | Sinking fund factor |
| HDH | Humidification Dehumidification | T | Temperature oC |
| I | Interest per year % | TDS | Total dissolved solids |
| M | Annual Yield Liter/year | WDS | Water desalination system |
| | Subscripts | | Greek letter symbols |
| Amb | Ambient | η | Efficiency |
| Atm | Atmospheric | ω | Specific humidity of dry air |
| Cw | Cooling water | | |
| Dw | Desalinated Water | | |
| Hw | Hot water | | |
| Sw | Sea Water | | |

Acknowledgments

The author I.N would like to acknowledge Mechanical engineering department – faculty of engineering for support to achieve this work. Additionally, the author would like to extend his acknowledgment to both faculty of agriculture and Faculty of Veterinary Medicine for their efforts in measurements and calibration of the tested samples.

Credit Authorship Contribution Statement

I.N has contribution to his work through; Methodology, Software, conceptualization, Data curation, Formal analysis Writing - original draft; Writing - review & editing; **AMA**: Supervision ,conceptualization, supervision, Methodology; Project administration , Writing - review & editing, Visualization; **T.N**: Supervision; **A.I**: Supervision ,conceptualization, supervision, Methodology; Project administration , Writing - review & editing, Visualization; **M.K.M.D**: Supervision , conceptualization, supervision, Methodology; Project administration , Writing - review & editing, Validation , Visualization, Data curation; Formal analysis

How to Cite this Article:

Nabil, I.M. *et al.* (2025) 'Investigation of Humidification Dehumidification Water Desalination Integrated with Fogging Technique', *Suez Canal Engineering, Energy and Environmental Science Journal*, 3(1), pp. 43–64.

Declaration of competing Interest

The authors declare that they have no known competing financial interests or personal relationships that could have appeared to influence the work reported in this paper.

Declaration of Funding

Funding: This work was not supported by or getting fund from any person or organization.

References: -

- Abemethy, R., Benedict, R., & Dowdell, R. (1983). *ASME measurement uncertainty*, ASME.
- Abu El-Maaty, A. E., Awad, M. M., Sultan, G. I., & Hamed, A. M. (2023). Innovative Approaches to Solar Desalination: A Comprehensive Review of Recent Research. *Energies*, 16(9). <https://doi.org/10.3390/en16093957>
- Alkhulafifi, Y. M., Baata, E., Al-Sulaiman, F. A., Ibrahim, N. I., & Ben-Mansour, R. (2021). Performance and exergoeconomic assessment of a novel combined ejector cooling with humidification-dehumidification (HDH) desalination system. *Desalination*, 500, 114843.
- Alrbai, M., Enizat, J., Hayajneh, H., Qawasmeh, B., & Al-Dahidi, S. (2022). Energy and exergy analysis of a novel humidification-dehumidification desalination system with fogging technique. *Desalination*, 522, 115421.
- Alrbai, M., Hayajneh, H. S., Al-Dahidi, S., & Alahmer, A. (2022). Thermodynamics analysis of a lab scale humidification-dehumidification desalination system employing solar energy and fogging approach. *Solar Energy*, 247, 397-407. <https://doi.org/10.1016/j.solener.2022.10.048>
- Amran, Y. A., Amran, Y. M., Alyousef, R., & Alabduljabbar, H. (2020). Renewable and sustainable energy production in Saudi Arabia according to Saudi Vision 2030; Current status and future prospects. *Journal of Cleaner Production*, 247, 119602.
- Chen, Q., Thu, K., Bui, T., Li, Y., Ng, K. C., & Chua, K. (2016). Development of a model for spray evaporation based on droplet analysis. *Desalination*, 399, 69-77.
- Chiranjeevi, C., & Srinivas, T. (2016). Influence of vapor absorption cooling on humidification-dehumidification (HDH) desalination. *Alexandria Engineering Journal*, 55(3), 1961-1967.
- Chiranjeevi, C., & Srinivas, T. (2017). Augmented desalination with cooling integration. *International Journal of Refrigeration*, 80, 106-119.
- Delyannis, E., & Delyannis, A. (1985). Economics of solar stills. *Desalination*, 52(2), 167-176.
- Doornbusch, G., van der Wal, M., Tedesco, M., Post, J., Nijmeijer, K., & Borneman, Z. (2021). Multistage electro dialysis for desalination of natural seawater. *Desalination*, 505, 114973. <https://doi.org/https://doi.org/10.1016/j.desal.2021.114973>
- Eke, J., Yusuf, A., Giwa, A., & Sodiq, A. (2020). The global status of desalination: An assessment of current desalination technologies, plants and capacity. *Desalination*, 495, 114633. <https://doi.org/https://doi.org/10.1016/j.desal.2020.114633>
- El-Maaty, A. E. A., Awad, M. M., & Qureshi, B. A. (2024). Exergy and energy analysis of a novel solar powered fog desalination system. *Desalination*, 569, 117057.
- El-Maaty, A. E. A., Awad, M. M., Sultan, G. I., & Hamed, A. M. (2019). Solar powered fog desalination system. *Desalination*, 472, 114130.
- Elbassoussi, M. H., Ahmed, M., Zubair, S. M., & Qasem, N. A. (2021). On a thermodynamically-balanced humidification-dehumidification desalination system driven by a vapor-absorption heat pump. *Energy Conversion and Management*, 238, 114142.
- Essa, F. A., Othman, M. M., Abdullah, A. S., Abou Al-Sood, M. M., & Omara, Z. M. (2024). Critical issues on advancements and challenges in HDH desalination units. *Results in Engineering*, 22, 102180. <https://doi.org/https://doi.org/10.1016/j.rineng.2024.102180>
- Fath, H. E., El-Samanoudy, M., Fahmy, K., & Hassabou, A. (2003). Thermal-economic analysis and comparison between pyramid-shaped and single-slope solar still configurations. *Desalination*, 159(1), 69-79.
- Gude, V. G. (2016). Desalination and sustainability—an appraisal and current perspective. *Water research*, 89, 87-106.
- Jamil, M. A., Elmutasim, S. M., & Zubair, S. M. (2018). Exergo-economic analysis of a hybrid humidification dehumidification reverse osmosis (HDH-RO) system operating under different retrofits. *Energy Conversion and Management*, 158, 286-297.
- Jia, X., Klemeš, J. J., Varbanov, P. S., & Wan Alwi, S. R. (2019). Analyzing the Energy Consumption, GHG Emission, and Cost of Seawater Desalination in China. *Energies*, 12(3), 463. <https://www.mdpi.com/1996-1073/12/3/463>

How to Cite this Article:

Nabil, I.M. et al. (2025) 'Investigation of Humidification Dehumidification Water Desalination Integrated with Fogging Technique', *Suez Canal Engineering, Energy and Environmental Science Journal*, 3(1), pp. 43–64.

- Khairat Dawood, M. M., Amer, A., Teamah, M. A., Aref, A., & Mansour, T. (2021). Experimental investigation of two-stage humidification-dehumidification desalination system integrated with an innovative oxy-hydrogen (HHO) system. *International journal of energy research*, 45(6), 9116-9140.
- Korepanov, A., Lekomtsev, P., & Niyazov, A. (2020). Energy characteristics of induction water heater. IOP Conference Series: Earth and Environmental Science,
- Lawal, D. U., & Qasem, N. A. (2020). Humidification-dehumidification desalination systems driven by thermal-based renewable and low-grade energy sources: A critical review. *Renewable and Sustainable Energy Reviews*, 125, 109817.
- Mohamed, A., Ahmed, M. S., Maghrabie, H. M., & Shahdy, A. G. (2021). Desalination process using humidification–dehumidification technique: A detailed review. *International journal of energy research*, 45(3), 3698-3749.
- Nabil, I., Abdalla, A. M., Mansour, T. M., Shehata, A. I., & Dawood, M. M. K. (2023). Salinity impacts on humidification dehumidification (HDH) desalination systems: review. *Environmental Science and Pollution Research*, 31(2), 1907-1925. <https://doi.org/10.1007/s11356-023-31327-5>
- Rosegrant, M. W., & Cai, X. (2002). Global water demand and supply projections: part 2. Results and prospects to 2025. *Water International*, 27(2), 170-182.
- Santosh, R., Arunkumar, T., Velraj, R., & Kumaresan, G. (2019). Technological advancements in solar energy driven humidification-dehumidification desalination systems-A review. *Journal of Cleaner Production*, 207, 826-845.
- Sharqawy, M. H., Antar, M. A., Zubair, S. M., & Elbashir, A. M. (2014). Optimum thermal design of humidification dehumidification desalination systems. *Desalination*, 349, 10-21.
- Shehata, A. I., Kabeel, A. E., Khairat Dawood, M. M., Abo Elazm, M. M., Abdalla, A. M., & Mehanna, A. (2019). Achievement of humidification and dehumidification desalination system by utilizing a hot water sprayer and ultrasound waves techniques. *Energy Conversion and Management*, 201. <https://doi.org/10.1016/j.enconman.2019.112142>
- Zheng, H. (2017). *Solar energy desalination technology*. Elsevier.

How to Cite this Article:

Nabil, I.M. et al. (2025) 'Investigation of Humidification Dehumidification Water Desalination Integrated with Fogging Technique', *Suez Canal Engineering, Energy and Environmental Science Journal*, 3(1), pp. 43–64.